



Ventrolateral Motor Thalamus Abnormal Connectivity in Essential Tremor Before and After Thalamotomy: A Resting-State Functional Magnetic Resonance Imaging Study

Constantin Tuleasca^{1,2,4,5}, Elena Najdenovska², Jean Régis⁶, Tatiana Witjas⁷, Nadine Girard⁸, Jérôme Champoudry⁶, Mohamed Faouzi⁹, Jean-Philippe Thiran³⁻⁵, Meritxell Bach Cuadra^{2,4}, Marc Levivier^{1,5}, Dimitri Van De Ville^{10,11}

■ OBJECTIVE: To evaluate functional connectivity (FC) of the ventrolateral thalamus, a common target for drug-resistant essential tremor (ET), resting-state data were analyzed before and 1 year after stereotactic radiosurgical thalamotomy and compared against healthy controls (HCs).

■ METHODS: In total, 17 consecutive patients with ET and 10 HCs were enrolled. Tremor network was investigated using the ventrolateral ventral (VLV) thalamic nucleus as the region of interest, extracted with automated segmentation from pretherapeutic diffusion magnetic resonance imaging. Temporal correlations of VLV at whole brain level were evaluated by comparing drug-naïve patients with ET with HCs, and longitudinally, 1 year after stereotactic radiosurgical thalamotomy. 1 year thalamotomy MR signature was always located inside VLV and did not correlate with any of FC measures ($P > 0.05$). This suggested presence of longitudinal changes in VLV FC independently of the MR signature volume.

■ RESULTS: Pretherapeutic ET displayed altered VLV FC with left primary sensory-motor cortex, pedunculopontine nucleus,

dorsal anterior cingulate, left visual association, and left superior parietal areas. Pretherapeutic negative FC with primary somatosensory cortex and pedunculopontine nucleus correlated with poorer baseline tremor scores (Spearman = 0.04 and 0.01). Longitudinal study displayed changes within right dorsal attention (frontal eye-fields and posterior parietal) and salience (anterior insula) networks, as well as areas involved in hand movement planning or language production.

■ CONCLUSIONS: Our results demonstrated that patients with ET and HCs differ in their left VLV FC to primary somatosensory and supplementary motor, visual association, or brainstem areas (pedunculopontine nucleus). Longitudinal changes display reorganization of dorsal attention and salience networks after thalamotomy. Beside attentional gateway, they are also known for their major role in facilitating a rapid access to the motor system.

Key words

- Essential tremor
- fMRI
- Motor thalamus
- Resting state
- Stereotactic radiosurgery
- Thalamotomy
- Ventrointermediate nucleus

Abbreviations and Acronyms

- ADL:** Activities of daily living
BA: Brodmann area
DBS: Deep-brain stimulation
DWI: Diffusion-weighted imaging
ET: Essential tremor
FC: Functional connectivity
FEW: Family-wise correction
fMRI: Functional magnetic resonance imaging
HC: Healthy control
HIFU: High-focused ultrasound
ION: Inferior olivary nucleus
MRI: Magnetic resonance imaging
RS: Radiosurgery
SD: Standard deviation
SRS-T: Stereotactic radiosurgical thalamotomy

Vim: Ventrointermediate nucleus

VLV: Ventral lateral ventral (thalamic nucleus)

From the ¹Neurosurgery Service and Gamma Knife Center, Centre Hospitalier Universitaire Vaudois, Lausanne, Switzerland; ²Medical Image Analysis Laboratory (MIAL) and Department of Radiology-Center of Biomedical Imaging (CIBM), Centre Hospitalier Universitaire Vaudois and University of Lausanne, Lausanne, Switzerland; ³Department of Radiology, Centre Hospitalier Universitaire Vaudois, Lausanne, Switzerland; ⁴Signal Processing Laboratory (LTS 5), Ecole Polytechnique Fédérale de Lausanne (EPFL), Lausanne, Switzerland; ⁵Faculty of Biology and Medicine, University of Lausanne, Lausanne, Switzerland; ⁶Stereotactic and Functional Neurosurgery Service and Gamma Knife Unit, and ⁷Neurology Department, CHU Timone, Marseille, France; ⁸AMU, CRMBM UMR CNRS 7339, Faculté de Médecine and APHM, Hôpital Timone, Department of Diagnostic and Interventional Neuroradiology, Marseille, France; ⁹Centre for Clinical Epidemiology, Institute of Social and Preventive Medicine, Lausanne, Switzerland; ¹⁰Faculty of Medicine, University of Geneva, Geneva, Switzerland; and ¹¹Medical Image Processing Laboratory, Ecole Polytechnique Fédérale de Lausanne (EPFL), Lausanne, Switzerland

To whom correspondence should be addressed: Constantin Tuleasca, M.D., M.D.-Ph.D. candidate; Dimitri Van de Ville, Ph.D.

[E-mail: constantin.tuleasca@gmail.com; dimitri.vandeville@epfl.ch]

Elena Najdenovska and Jean Régis are co-first authors.

Citation: World Neurosurg. (2018) 113:e453-e464.

<https://doi.org/10.1016/j.wneu.2018.02.055>

Journal homepage: www.WORLDNEUROSURGERY.org

Available online: www.sciencedirect.com

1878-8750/\$ - see front matter © 2018 Elsevier Inc. All rights reserved.

INTRODUCTION

Essential tremor (ET) is the most prevalent movement disorder in the adult population.^{1–3} Initially regarded as an individual illness, it is nowadays suggested as a family of diseases.⁴ The pathophysiology is still poorly understood.^{3,5}

One hypothesis for tremor generation suggests a central role of the inferior olivary nucleus (ION).⁶ In addition, recent findings using resting-state functional magnetic resonance imaging (fMRI) showed that pretherapeutic interconnectivity strength between the ION and bilateral motor cortex is predictive for tremor arrest after thalamotomy.⁷ This hypothesis is based on the fact that ION would produce an abnormal rhythmic output, affecting synchronization of Purkinje cell firing,⁸ propagated through the cerebellothalamic tract,^{9,10} tuning motor activity.¹¹ Independently of the tremor origin (ION vs. cerebellum), the abnormal rhythmic output travels from dentate cerebellar nucleus to the contralateral M1 area, passing through the ventrointermediate nucleus (Vim) (e.g., “tremor ax”).¹² In fact, the Vim has been successfully targeted in tremor since the pioneering thermocoagulation performed by Hassler,¹³ further continuing with the stereotactic radiofrequency thalamotomy¹⁴ and more recently deep-brain stimulation (DBS),^{15,16} the standard of care.

An alternative to open surgical procedures, radiosurgery (RS), which aims at the same target (e.g., Vim), has a high level of evidence.^{17–19} Unlike radiofrequency thalamotomy and DBS, RS does not have the possibility of intraoperative confirmation and induces a delayed clinical and radiologic effect, up to 1 year after the procedure.¹⁷ More recently, high-focused ultrasound (HIFU), which produces a controlled thermocoagulation, has demonstrated its safety and efficacy, with an immediate clinical and radiologic effect.²⁰

fMRI is a valuable, noninvasive technique, that allows exploring brain networks in healthy and pathologic conditions, including ET.^{21–24} Resting-state fMRI, in particular, evaluates interactions between segregated brain areas in the absence of an explicit task. Resting-state activity is observed through changes in spontaneous fluctuations of blood-oxygen-level-dependent signal.²⁵ The former can be acquired with minimal patient compliance, which unlocks new possibilities for application in the clinical realm.²⁶

Here, we used resting-state fMRI to describe the anterolateral motor thalamus temporal correlations at the whole brain level (seed-to-voxel analysis). Function connectivity (FC) derived from resting-state fMRI time-courses was analyzed pretherapeutically, before stereotactic radiosurgical thalamotomy (SRS-T, as compared with healthy controls [HCs]) and 1 year later. The studied region-of-interest seed was the ventrolateral ventral nucleus (VLV; nomenclature form Morel et al.²⁷), as Vim is not directly visible on current 1.5- and 3-Tesla magnetic resonance imaging (MRI) acquisitions. The VLV was obtained by using a newly automated, robust, and reproducible method for thalamus clustering published by our group.²⁸ This method exclusively explores local thalamic diffusion properties across both HCs and patients with ET (pretherapeutic data).²⁸

Our primary aims in this study were 1) to compare VLV FC in HCs versus pretherapeutic ET; and 2) to evaluate longitudinal changes 1 year after SRS-T (as compared with pretherapeutic), to account for the delayed clinical effect.²⁹

Our first hypothesis was that pretherapeutically FC is impaired within the previously described tremor network, based on recent

fMRI studies and existing physiopathologic theories.^{1,22,23} However, in addition to the main role of Vim in tremor propagation and its altered thalamocortical connectivity in ET,²³ recent studies have specified an increased FC of sensory-motor and salience networks in patients with ET compared with HCs.³⁰ Our second hypothesis was that SRS-T would not only generate changes within the thalamocortical network but also produce a functional reorganization of salience networks.

MATERIALS AND METHODS

Participants

We included 17 consecutive patients (right-handed, drug-resistant, drug-naïve during study neuroimaging protocol) treated only with left unilateral SRS-T between September 2014 and August 2015 at Marseille University Hospital, Marseille, France. All were referred by a neurologist specialized in movement disorders (T.W.). Clinical diagnosis was ET in all cases.

Only patients meeting inclusion criteria analyzed here were included: confirmed diagnosis of ET, able to give formal approval, drug-resistance after adequate trials, age between 18 and 80 years, and targeted thalamic area apparent on pretherapeutic MRI. Patients with mixed or Parkinsonian tremor were excluded, as well as those with previous contralateral SRS-T, epilepsy, brain tumors, or stroke. The main indication for SRS-T rather than DBS/stereotactic thalamotomy was medical comorbidities, advanced age, or patient refusal of DBS. Ten HCs (age- and sex-matched) also were enrolled (age: mean 70.4 years; median 71 years; range 59–83 years; male to female ratio: 4:6).

Standard Protocol Approvals, Registrations, and Patient Consents

The Ethical Committee of the Timone University Hospital (CPPRB 1) provided formal approval. Written informed consent was obtained for all cases. The ongoing trial started in September 2014.

Tremor and Cognitive Assessment

Tremor severity was assessed with the questionnaire designed by Bain et al.³¹ (e.g., activities of daily living [ADL])³¹ and tremor score on the right-treated hand from the Fahn-Tolosa-Marin Tremor Rating Scale.³² Tremor assessment was standardly performed at baseline and 1 year after SRS-T to account for delayed clinical effect.²⁹

Cognitive assessment was performed with the Mattis Dementia Rating Scale³³ and was not statistically different before (mean 135.9) and 1 year after SRS-T (mean 135.5, $P > 0.05$).

Stereotactic Radiosurgical Thalamotomy Procedure

Stereotactic radiosurgical thalamotomy was performed by the same neurosurgeon (J.R.). After application of the Leksell Coordinate Frame G (Elekta AB, Stockholm, Sweden), under local anesthesia,²⁹ all patients underwent both stereotactic computed tomography and MRI. Indirect targeting was performed in all cases with the use of uniform and standard methodology by Guiot's diagram, placed 2.5 mm above the anterior commissure–posterior commissure line and 11 mm lateral to the wall of the third ventricle. A single 4-mm isocenter was used, and a maximal prescription dose of 130 Gy.

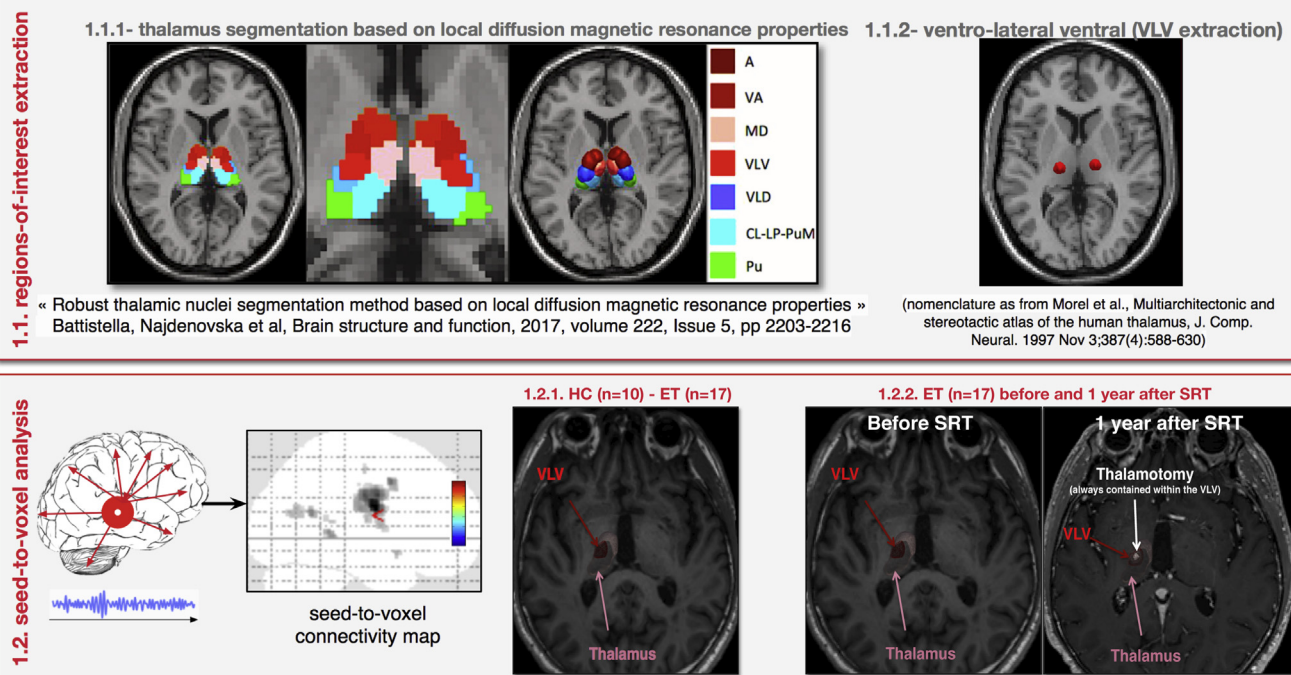


Figure 1. Schematic illustration of the data approach. **(1.1.)** Thalamus segmentation is done with our previously published methodology and further ventral lateral ventral (VLV) is extracted as a region of interest for subsequent seed-to-voxel analysis. **(1.2.)** Seed-to-voxel connectivity maps are obtained in healthy controls (HC; **1.2.1.**) and in patients with essential tremor (ET) before and after stereotactic radiosurgical thalamotomy (SRT); the thalamotomy (in white) is coregistered with the VLV (in red) and was always present inside the cluster (**1.2.2.**). VA, ventral anterior; MD,

medio-dorsal; VLD, ventral-lateral dorsal; CL-LP-PuM, central lateral-lateral posterior-pulvinar medial; Pu, pulvinar. The image appearing in **Figure 1.1.1.** is an adapted version of the Figures 4 and 5 from our paper “Battistella G, et al. Robust thalamic nuclei segmentation method based on local diffusion magnetic resonance properties. *Brain Struct Funct* 2017;222:2203-2216²⁸;” the figure has been adapted under the terms of the Creative Commons Attribution 4.0 International License (<http://creativecommons.org/licenses/by/4.0/>).

Image Acquisition

Pretherapeutic neuroimaging included structural noninjected T1-weighted MRI, diffusion-weighted imaging (DWI), and resting-state fMRI. Post-therapeutic neuroimaging at 1 year after SRS-T included structural gadolinium-injected T1-weighted (for better visualization of thalamotomy MR signature) and resting-state fMRI.

Neuroimaging was done on a head-only 3T MRI scanner (Siemens Medical Solutions, Erlangen, Germany) with a 32-channel receive-only phased-array head coil. The following parameters were employed: for the high-resolution structural, a 3D T1-weighted, repetition time/echo time = 2300/2.98 milliseconds, isotropic voxel of 1 mm³, 160 slices; DWI was acquired with 72 gradient directions and b = 1000 s/mm²; T2*-weighted fast echo planar imaging (blood-oxygen-level-dependent contrast): repetition time/echo time = 3.3 seconds/30 milliseconds/90°, voxel size 4 × 4 × 4 mm, 300 volumes acquired per subject, 46 interleaved axial slices. Same parameters were applied in HC (including for DWI and resting-state fMRI).

The resting-state fMRI experiments, acquired with no explicit task, consisted of a 10-minute run in which participant were asked to relax with their eyes closed without falling asleep or engaging in cognitive or motor tasks. Patients and HC were monitored during scanning to ensure maintenance of the eyes-closed and the awake state.

Resting-State fMRI Preprocessing

Neuroimaging data were analyzed in Lausanne (Switzerland) by persons not involved in patient selection, treatment, or post-therapeutic evaluation (C.T., E.N., M.B.C., and D.V.D.V.). Processing of fMRI data was performed with the use of different standard software suites: SPM12 (<http://www.fil.ion.ucl.ac.uk/spm/>, London, United Kingdom) implemented in MATLAB R2016a (Mathworks, Natick, Massachusetts, USA), FSL (FMRIB Software Library v5.0. Analysis Group, FMRIB, Oxford, United Kingdom), and FreeSurfer (Massachusetts General Hospital, Boston, Massachusetts, USA). The preprocessing pipeline of the fMRI data encompassed standard procedures, including motion correction (FSL McFlirt function) with selection of the middle fMRI image as the reference one, correction of geometric distortions using the individual field map, signal stabilization, coregistration of the T1-to-fMRI, spatial smoothing (full width at half maximum = 3 mm), temporal band pass filtering (0.01–0.10 Hz), and regression of the average signals from both the white matter and the cerebrospinal fluid.

Resting-State fMRI Frame Censoring, of Particular Importance for Patients with ET

Head motion during the MRI acquisitions, even if of submillimetric amplitude, has been already demonstrated as

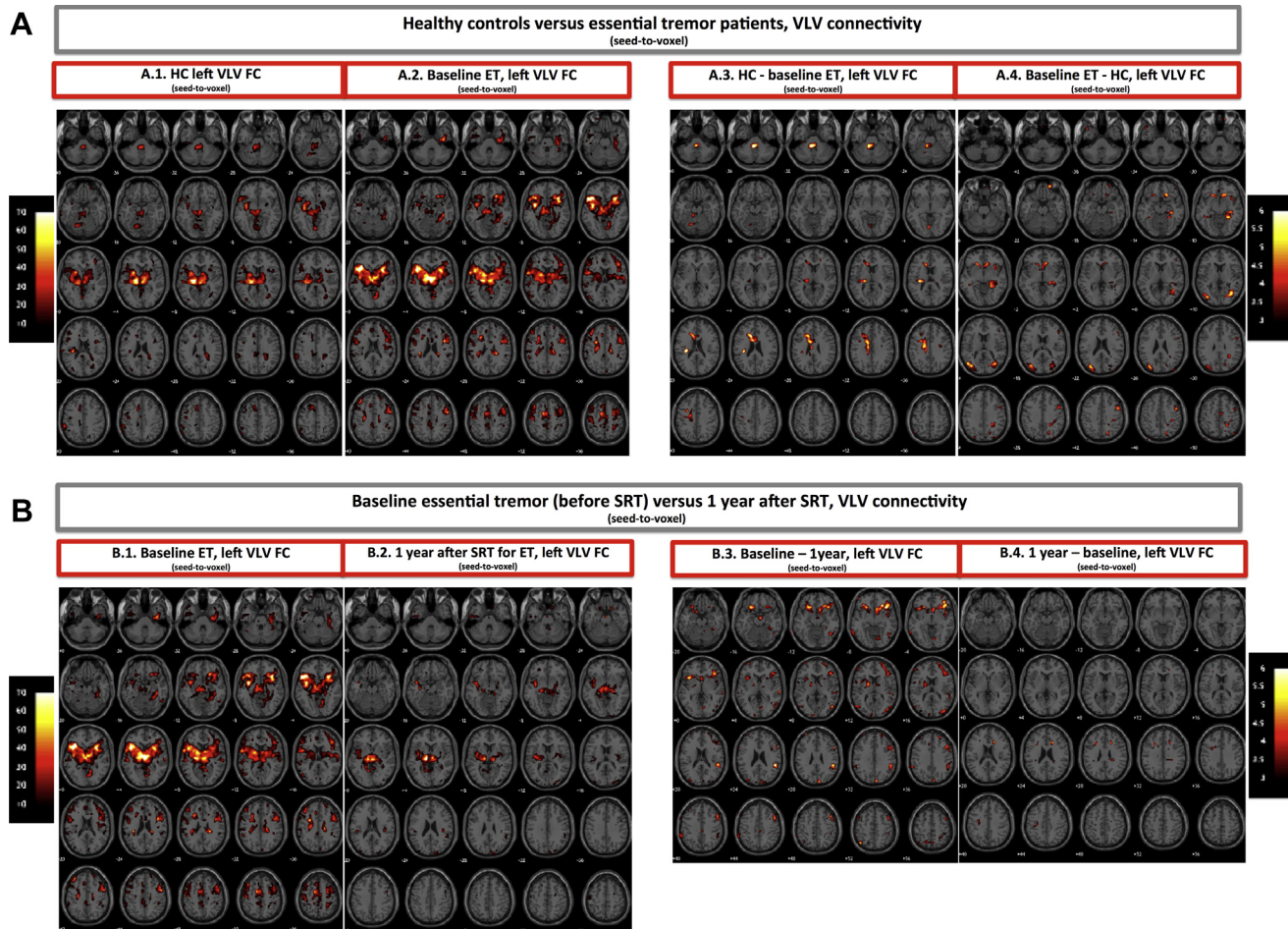


Figure 2. Illustration of the left ventral lateral ventral (VLV) functional connectivity (FC) in healthy controls (HCs) versus patients with essential tremor (ET). **(A.A.1.)** HC. **(A.A.2.)** Pretherapeutic ET. **(A.A.3.)** HCs, pretherapeutic ET. **(A.A.4.)** Pretherapeutic ET – HC; illustration of the left

VLV FC pretherapeutically and 1 year after stereotactic radiosurgical thalamotomy (SRS-T). **(B.B.1.)** Pretherapeutic ET. **(B.B.2.)** One year after SRS-T. **(B.B.3.)** Pretherapeutic – 1 year after SRS-T. **(B.B.4.)** One year after SRS-T – pretherapeutic.

nonphysiological source of spurious brain connectivity in resting-state fMRI data.³⁴ We computed Power's framewise displacement index for each time point.³⁴ When it exceeded 0.5 mm, the corresponding frame was “scrubbed” along with 2 proceeding and 2 following ones (for a total of 5 for one time-point exceeding the upper limit allowed). Only the remaining frames were further considered for analysis. Here, the mean number of frames taken out was 35 (median 15, range 0–135).

Resting-State fMRI Data Analysis

For both left and right VLV, FC maps were generated individually using the REST³⁵ by a seed-to-voxel approach. Furthermore, they were normalized applying the Montreal Neurological Institute template using SPM 12 (London, United Kingdom).

The resulting subject-level spatial maps were statistically analyzed with SPM 12, using: 1) 2-sample t test for evaluating the

left versus the right VLV FC; 2) 2-sample t test for assessing HC versus ET; and 3) paired t test for evaluating the FC between pretherapeutic and 1 year after SRS-T. We first applied an uncorrected height threshold of $P < 0.001$ followed by a $P < 0.05$ family-wise correction (FWE)- or false discovery rate–corrected cluster-size threshold. All the presented graphs (including boxplots and scatter plots) were made with Stata (version 11, StataCorp LLC, College Station, Texas, USA). The DWI analysis and thalamus segmentation can be seen in **Figure 1, 1.1. (1.1.1. and 1.1.2.; Supplementary Materials)**.

Automated 3T diffusion MRI-Based VLV Segmentation

A short and simplified overview of DWI analysis and thalamus segmentation can be seen in **Figure 1, 1.1. (1.1.1. and 1.1.2.)** and within the **Supplementary Materials**.

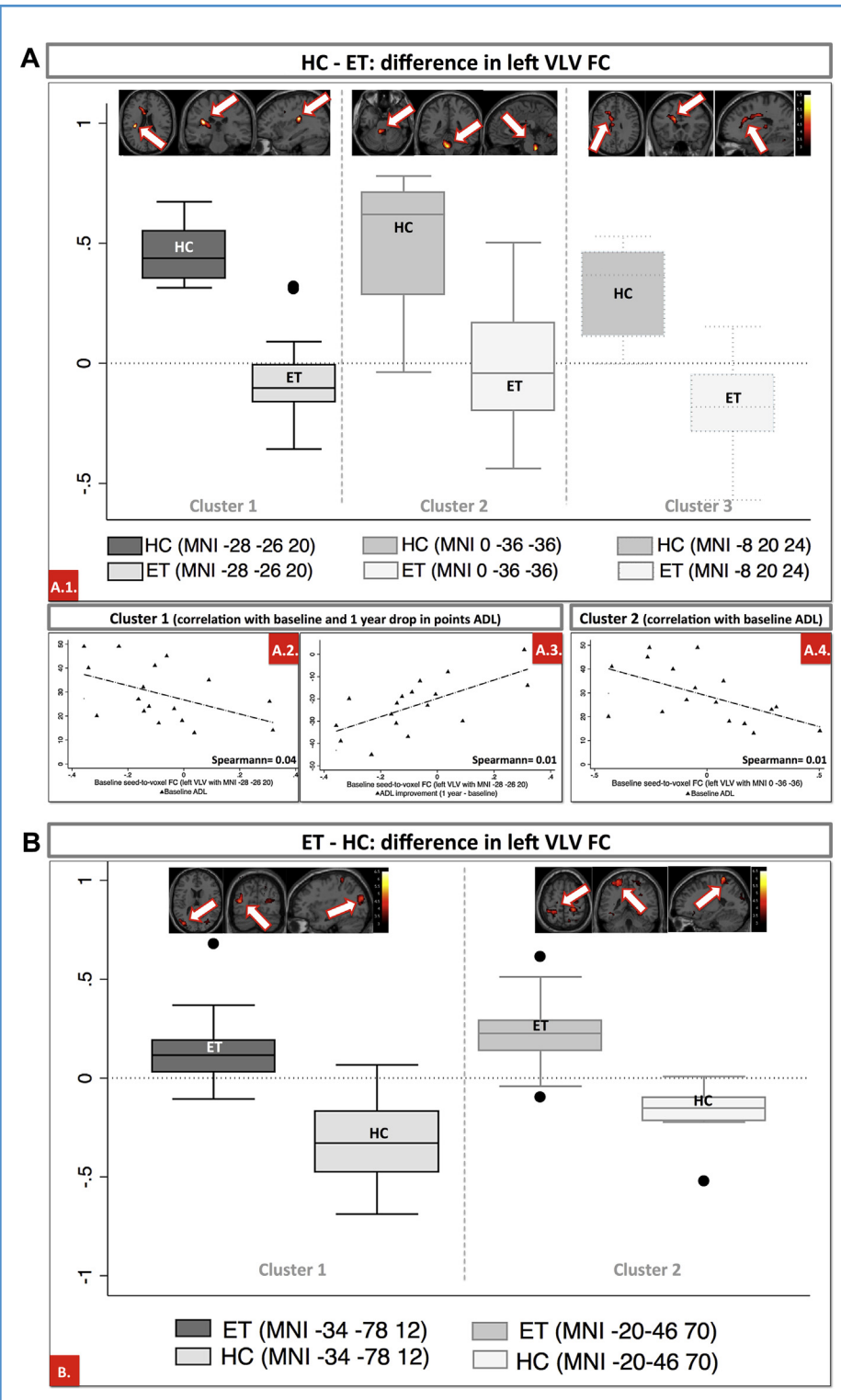


Figure 3. Illustration of differences of left ventral lateral ventral (VLV) seed-to-voxel function connectivity (FC) values for the statistically significant clusters in (A) healthy controls (HC) – pretherapeutic essential tremor (ET): somatosensory cortex (A.1., left, cluster 1), pedunculopontine nucleus (A.1., center, cluster 2), and Brodmann area 32 (A.1., right, cluster 3); and (B) ET – HC: right occipital association cortex (B, cluster 1) and posterior parietal regions (B, cluster 2); all boxplots display the minimum, maximum, and median values.

FC within somatosensory area correlates with baseline activities of daily living (ADL; A.2.) and with ADL (A.3.); FC within pedunculopontine nucleus correlates with baseline ADL (A.4.). (B) Pretherapeutic ET – HC: right occipital association cortex (B, cluster 1) and posterior parietal regions (B, cluster 2); all boxplots display the minimum, maximum, and median values.

Lesion Location After Thalamotomy

The classical “ring-enhancing” MR signature,²⁹ visualized 1 year after SRS-T, was always located inside the left VLV³⁶ cluster (**Figure 1, 1.2., 1.2.1., 1.2.2.**).

Clinical Characteristics

Mean age was 70.1 years (range 49–82; 5 males, 12 females). Mean duration of symptoms was 38 years (range 6–70 years). The mean baseline ADL was 29.1 (standard deviation [SD] 12, range 13–49). The mean decrease in points at 1 year after SRS-T was –23.06 (SD 11.9, range 2 to –45). The mean baseline tremor score on the treated hand was 18.6 (SD 5.5, range 8–30). The mean decrease in points at 1 year after SRS-T was –11.4 (SD 4.1, range –4 to –19). The mean time to tremor improvement was 3.32 months (SD 2.7, range 0.5–10 months).

Radiologic Characteristics: Thalamotomy Volume

The 1 year thalamotomy MR signature volume has been drawn on T1 (gadolinium-injected) MR 1 year after SRS-T, which is considered the definitive radiologic answer in our experience.¹⁹ To ensure the accuracy of volume calculation, each patient’s MRI at 1-year follow-up was imported in the Leksell GammaPlan software (Elekta AB) and coregistered with the therapeutic images. We projected on the MR-signature the 90-Gy isodose line, which corresponds to the final radiologic response, in our previously published experience.^{19,37} Manually, with the segmentation tools, the draw was made for the individual cases. The “volume” module inside the station was used to extract the values.

The mean 1 year thalamotomy MR signature volume after SRS-T was 0.125 mL (SD 0.162, range 0.002–0.600 mL). There was no correlation between decrease in ADL or head tremor improvement and lesion volume ($P > 0.05$), but the former related with tremor score on the treated hand drop ($P = 0.01$). The FC values within the relevant clusters showed no statistically significant correlation with lesion volume ($P > 0.05$).

RESULTS

We evaluated the impact of age, disease duration, or volume lesion, and we report no statistically significant correlation (Spearman > 0.05) with FC values. Furthermore, no statistically significant differences in FC between left and right VLV nucleus were found.

VLV FC in Pretherapeutic Drug-Naïve Patients with ET

Drug-naïve patients with ET, compared with HCs (**Figure 2A, A.1.–A.4., Figure 3A** and **B**, and **Table 1**) showed decreased (median negative value) FC between the left VLV and the following clusters: left primary somatosensory area (inferior part, $p_{FWE\text{-cor}} = 0.035$), pedunculopontine nucleus ($p_{FWE\text{-cor}} = 0.003$), and dorsal anterior cingulate cortex (Brodmann area [BA] 32, $p_{FWE\text{-cor}} = 0.000$; **Figure 3, A.1.; Table 1**). Furthermore, a decreased pretherapeutic FC with the primary somatosensory cortex (Spearman = 0.04; **Figure 3, A.2.; Table 1**) and pedunculopontine nucleus (Spearman = 0.01; **Figure 3, A.4.**) correlated with baseline ADL. A decrease in points of ADL 1 year after SRS-T correlated with an increase in FC between left VLV and primary somatosensory cortex (Spearman = 0.01, **Figure 3, A.3.; Table 1**).

Drug-naïve patients with ET, compared with HCs, revealed increased left FC with left visual association cortex (BA19, $p_{FWE\text{-cor}} = 0.005$) and left superior parietal regions (BA 7, $p_{FWE\text{-cor}} = 0.014$).

VLV FC at 1 Year After SRS-T

A decrease from pretherapeutic positive FC to a median value close to zero 1 year after SRS-T (**Figure 2, B.1.–B.4.; Figure 4, A.1.–A.4.; Table 1**) was found for the following clusters: right insular and orbitofrontal cortex (BA 47, $p_{FWE\text{-cor}} = 0.000$), right BA 40 (posterior parietal, supramarginal gyrus, $p_{FWE\text{-cor}} = 0.002$), left BA 13 (anterior insula, $p_{FWE\text{-cor}} = 0.000$), and right BA 44 and 8 (inferior frontal gyrus and frontal-eye fields, $p_{FWE\text{-cor}} = 0.002$). In contrast, an increase from pretherapeutic negative FC to a median close to zero 1 year after SRS-T is reported for left VLV FC with right supplementary motor area ($p_{uncor} = 0.015$; **Figure 4B** and **Table 1**).

DISCUSSION

In the present study, we evaluated the tremor network using a seed-to-voxel approach on resting-state fMRI data, as functional imaging had been widely used as an alternative for evaluating segregated brain processes.^{38,40} We focus on FC of the most commonly used surgical target for tremor, the ventrolateral motor thalamus. With regard to HCs versus pretherapeutic ET FC, we report as statistically significant: primary somatosensory, visual association, and anterior cingulate cortex, as well as pedunculopontine nucleus. The longitudinal changes 1 year after SRS-T relate to dorsal attention (frontal eye-fields and parts of the dorsal premotor cortex and posterior parietal areas^{41,42}) and salience (i.e., insula) networks. Additional FC changes are present within several distinct clusters: language-related areas (BA 47), meaning and phonology (BA 40), or selective response suppression in go/no-go tasks and hand movements areas (all for BA 44).

With regard to differences between HCs and patients with ET, previous resting-state fMRI studies have provided noteworthy findings. Buijink et al.²² used motor-task fMRI and electromyography and reported FC decrease in patients with ET between cortical and cerebellar motor regions. Gallea et al.⁴³ analyzed resting-state fMRI data and reported FC alterations in supplementary motor areas, which were considered consequence of a cerebellar defect and acting to attempt to reduce tremor in motor output by reducing communications with M1 hand areas. More recently, Fang et al.²³ used also a region-of-interest approach and evaluated time-courses of Vim. The authors reported FC increase between the Vim and M1 area, as well as a decrease with the cerebellum. Additional resting-state fMRI studies used other data-driven approaches.^{21,30}

We report multiple network alterations of left VLV pretherapeutic FC in patients with ET. At the cortical level, some of the representative regions have already been reported by previous studies. This includes the primary somatosensory/somatotmotor cortex,⁴⁴ which is responsible for integration of somatic sensation, visual stimuli, and movement planning,⁴⁵ or BA 32, involved in “Stroop” task.⁴⁶ We further report newly discovered FC alterations of the left VLV with left posterior parietal BA 7 and left visual association cortex BA 19. The BA 7 is involved in locating objects in the space and represents a point of convergence between vision and proprioception; its presence

Table 1. Overview of the Main Left VLV FC Results

Set-Level		Cluster-Level				Peak-Level				MNI, Anatomical Area	
P	pFWE-cor	pFDR-cor	k _c	puncor	pFWE-cor	pFDR-cor	T/P	Z _E	puncor	puncor	
HC—ET patients											
0.000	0.035	0.007	205	0.002	0.019	0.030	7.19	5.16	0.000	−28	−26 20, L sensory-mot
	0.003	0.001	332	0.000	0.187	0.109	5.93	4.57	0.000	0	−36 −36, peduncle-pontine
	0.000	0.000	648	0.000	0.250	0.113	5.76	4.48	0.000	−8	20 24, L BA 32
ET patients—HC											
0.000	0.005	0.008	314	0.000	0.676	0.566	5.04	4.10	0.000	−34	−78 12, L BA 19
	0.014	0.012	254	0.001	0.820	0.566	4.82	3.97	0.000	−20	−46 70, L BA 7
Pretherapeutic—1 year after SRS-T (ET patients)											
0.000	0.000	0.000	1099	0.000	0.217	0.783	7.23	4.68	0.000	42	24 −8, R BA 47
	0.002	0.001	298	0.000	0.341	0.783	6.80	4.53	0.000	56	−38 24, R BA 40
	0.000	0.000	660	0.000	0.571	0.783	6.25	4.32	0.000	−34	18 0, L BA 13
	0.002	0.001	289	0.000	0.952	0.784	5.29	3.92	0.000	48	16 34, R BA 44 and 8
1 year after SRS-T—pretherapeutic (ET patients)											
	0.308	0.105	85	0.015	0.883	0.583	5.55	4.03	0.000	22	24 22, R SMA

VLV, ventral lateral ventral; FC, functional connectivity; FWE, family-wise correction; cor, corrected; FDR, false discovery rate; uncor, uncorrected P value; T/P, height threshold; Z_E, Z score; MNI, Montreal Neurological Institute; HC, healthy control; ET, essential tremor; L, left; BA, Brodmann area; SRS-T, stereotactic radiosurgical thalamotomy; R, right; SMA, supplementary motor area.

suggests a functional alteration of sensorial networks in patients with ET. The left BA 19 presence is somewhat surprising, most probably by polysynaptic connections, and would express currently underestimated alterations of visual networks in patients ET.

We also report altered FC of the pedunculopontine nucleus, which is responsible for modulation of gait (initiation, maintenance, modulation, and other stereotyped motor behaviors). The pedunculopontine nucleus has been classically explored in DBS for patients with Parkinson disease with axial symptoms less responsive to subthalamic nucleus stimulation and is considered highly interconnected with the pallido-thalamo-cortical circuit.⁴⁷ In the context of patients with ET, alterations in FC between this structure and the motor thalamus are most probably related to other neurologic features, already acknowledged, mainly deficits on both balance (the ability to maintain the body within its base of support) and gait.⁴⁸ An additional argument in favor of this statement is the found correlation between pretherapeutic ADL and FC with this structure, being known that ADL is global score including also aspects related to gait and posture.

An added value of this report is the display of longitudinal changes in FC 1 year after SRS-T. For dorsal attention and salience network, FC exhibited a decrease from positive median values to ones close to zero after SRS-T. This would support the fact that pretherapeutic global increase in FC described by other authors in these networks³⁰ is an adaptive change during ET disease course. Thalamotomy done by RS is generating a progressive functional reorganization of these systems, with further decrease of an

originally probably adaptive and compensatory hyperactivity thought to balance tremor appearance and disease progression.

The same type of changes described in the previous 2 networks is applicable to the left VLV FC with anterior insula, which is involved in salience and warrants further attention. It is well acknowledged that the insula is the bottom-up detection of salient events, allowing switching between other large-scale networks to facilitate access to attention and working memory resources when a salient event is detected. Moreover and of high relevance, the anterior insula has a strong additional functional coupling with anterior cingulate cortex, facilitating rapid access to the motor system.⁴⁹ It would so act as an integral hub in the generation of appropriate behavioral responses to salient stimuli.⁴⁹ Sridharan et al.⁵⁰ revealed that the right anterior insula plays a critical and causal role in interchanging between 2 other major networks (central attention and default-mode network), known to demonstrate competitive interactions during cognitive information processing. Across stimulus modalities, this structure would play a critical and causal role in activating the central attention and deactivating the default-mode network.⁵⁰ These entire features would give the insula a balance capacity between salience and motor networks.

We also report FC changes with the right supplementary motor area, which has multiple roles, including postural stability during stance or walking, bimanual coordination, or the initiation of internally generated as opposed to stimulus driven movement.⁵¹

Only 2 previous resting-state fMRI studies, not related to RS,^{52,53} evaluated the effect of HIFU thermocoagulation on brain networks up to 3 months after the procedure. A major difference is

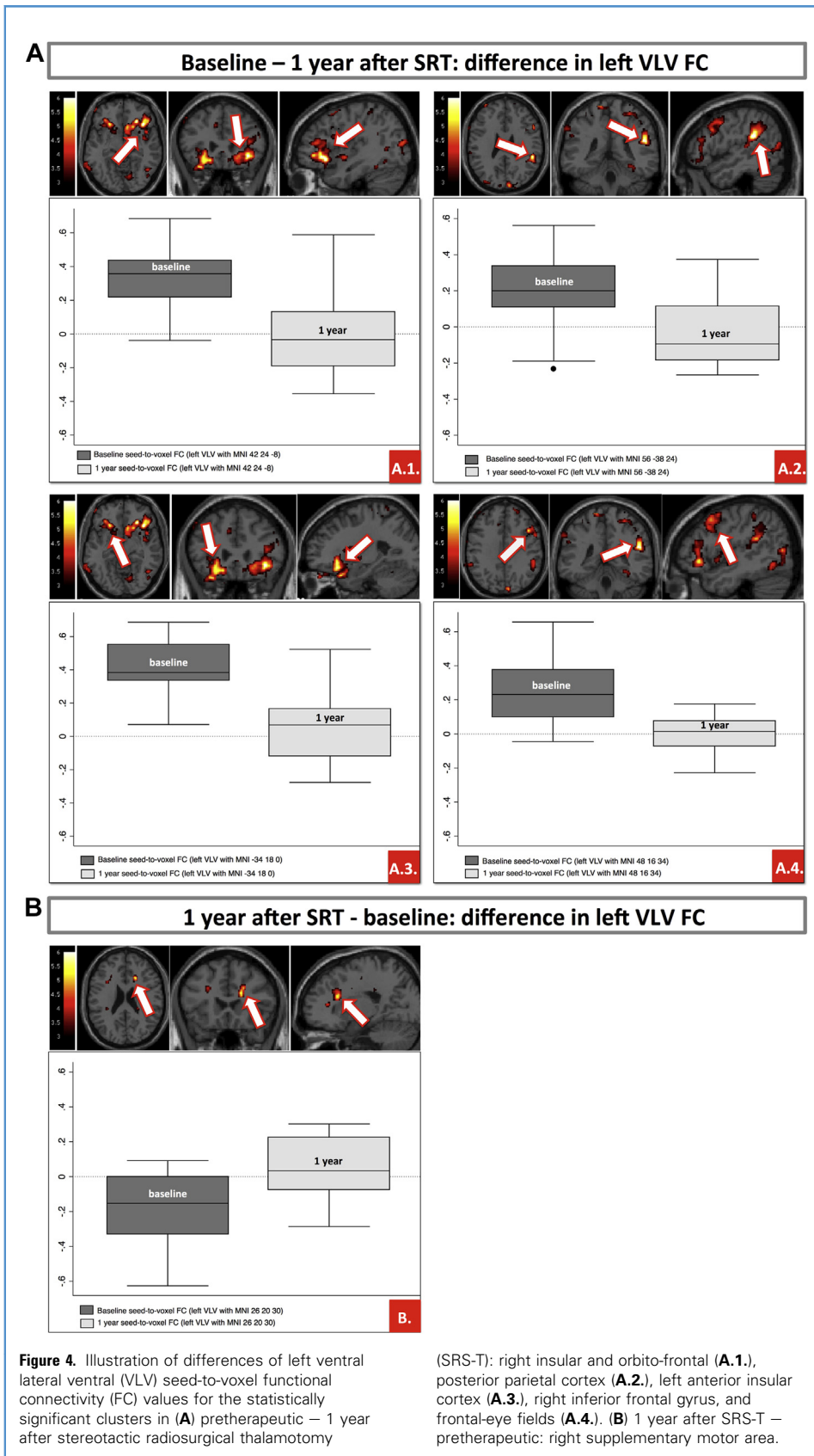


Figure 4. Illustration of differences of left ventral lateral ventral (VLV) seed-to-voxel functional connectivity (FC) values for the statistically significant clusters in (A) pretherapeutic – 1 year after stereotactic radiosurgical thalamotomy

(SRS-T): right insular and orbito-frontal (**A.1.**), posterior parietal cortex (**A.2.**), left anterior insular cortex (**A.3.**), right inferior frontal gyrus, and frontal-eye fields (**A.4.**). (B) 1 year after SRS-T – pretherapeutic: right supplementary motor area.

that HIFU, unlike RS, produces an apparent lesion and clinical effect immediately. The delayed effect of RS could account for brain networks reorganization and allow for plasticity.

It is currently considered that a dense network of axonal pathways interconnects structurally segregated and functionally specialized specific brain regions.⁵⁴ It has been advocated that structural connectivity patterns and functional interactions between different regions of cortex are meaningfully correlated.⁵⁴ Furthermore, strong FC commonly observed between regions with no direct structural connection.⁵⁵ FC changes might be also due to tissue disruption, with further involvement of the specific white matter tracts, eventually affected by Vim SRS-T. For instance, in patients with ET treated with HIFU, diffusion tensor imaging revealed changes over time not only at the thermocoagulation site, but also in distant areas of the brain. After corrections for multiple comparisons, only remote diffusion tensor imaging changes were correlated with the clinical improvement.⁵⁶ Functional studies using fluorodeoxyglucose—positron emission tomography also confirmed remote effects after Vim DBS in ET. These effects involved the cerebellum, in patients with posttherapeutic ataxia, suggesting thus possible clinical effects.⁵⁷

We have recently reported tremor recovery as related to distant sites changes after SRS-T using resting-state fMRI and whole-brain analysis without prior assumption (i.e., independent component analysis^{58,59}). We reported 2 networks that presented statistically significant interconnectivity with visual clusters: one included the bilateral motor network, frontal eye-fields, and left cerebellum lobule VI, of which interconnectivity strength with right visual BA 19 related to tremor arrest after SRS-T; the second included reminiscent of the salience network, which showed altered interconnectivity strength with right fusiform gyrus and V5.⁶⁰

Our study design has several potential limitations, although we have taken many precautions. One, related to study design, is the use of resting-state data, which might not be directly related to

motor performance; however, we aimed at studying network changes in the absence of a task. A second limitation is the small number of subjects. A third one is the lack of data on longitudinal changes (at 1 year) in the HC group; nevertheless, recent studies have advocated the reproducibility of functional networks across multiple sessions, including 1 year apart.⁶¹ Furthermore, the neurologic evaluation was not blinded. Also, at which exact time point SRS-T RS induces these changes in brain networks remains unknown. Another aspect is related to resting-state fMRI resolution. Regarding the former, tiny anatomical structures, such as the pedunculopontine nucleus, are reasonable to assume but illustrate this limitation.

In conclusion, the present resting-state fMRI analysis has allowed us, using longitudinal study after SRS-T, to depict for the first time FC reorganization of several major brain networks, which cannot be easily captured by other existing techniques. We postulate that the commonly targeted ventrolateral thalamus for drug-resistant ET would act as a mediator after the intervention, inducing major changes in dorsal attention, salience, and supplementary motor networks. The insula would act like a hub in downregulating the relationship between all these aforementioned structurally segregated, yet functionally highly interconnected, systems. Pretherapeutic hyperactivity of the attentional networks might be an adaptive change in ET during the disease course, as previously postulated by other authors. By SRS-T, it is generated a “functional reset” of these circuits, and they are brought back to a “normal state.” We postulate that a more pre-eminent insular role as well as of other structures related to attention exists, and this might further interact with motor-related systems for normal motor and cognitive homeostasis.

ACKNOWLEDGMENTS

We acknowledge the important contribution of Axelle Cretol, from Marseille University Hospital (CHU Timone), Marseille, France, who, as research assistant, kept the database up-to-date.

REFERENCES

1. Deuschl G, Elble R. Essential tremor—neurodegenerative or nondegenerative disease towards a working definition of ET. *Mov Disord*. 2009;24:2033-2041.
2. Louis ED. Clinical practice. Essential tremor. *N Engl J Med*. 2001;345:887-891.
3. Louis ED. Essential tremor. *Lancet Neurol*. 2005;4:100-110.
4. Louis ED. Essential tremors: a family of neurodegenerative disorders? *Arch Neurol*. 2009;66:1202-1208.
5. Sharifi S, Nederveen AJ, Booij J, van Rootselaar AF. Neuroimaging essentials in essential tremor: a systematic review. *Neuroimage Clin*. 2014;5:217-231.
6. Llinás RR. The olivo-cerebellar system: a key to understanding the functional significance of intrinsic oscillatory brain properties. *Front Neural Circuits*. 2013;7:96.
7. Tuleasca C, Najdenovska E, Régis J, Witjas T, Girard N, Champoudry J, et al. Pretherapeutic functional neuroimaging predicts tremor arrest after thalamotomy [e-pub ahead of print]. *Acta Neurol Scand* <https://doi.org/10.1111/ane.12891>, Accessed January 7 2018.
8. Hansel C. Reading the clock: how Purkinje cells decode the phase of olivary oscillations. *Neuron*. 2009;62:308-309.
9. Bhalsing KS, Saini J, Pal PK. Understanding the pathophysiology of essential tremor through advanced neuroimaging: a review. *J Neurol Sci*. 2013;335:9-13.
10. Passamonti L, Novellino F, Cerasa A, Chiriacò C, Rocca F, Matina MS, et al. Altered cortical-cerebellar circuits during verbal working memory in essential tremor. *Brain*. 2011;134:2274-2286.
11. Popa T, Russo M, Vidailhet M, Roze E, Lehéricy S, Bonnet C, et al. Cerebellar rTMS stimulation may induce prolonged clinical benefits in essential tremor, and subjacent changes in functional connectivity: an open label trial. *Brain Stimul*. 2013;6:175-179.
12. Middleton FA, Strick PL. Basal ganglia and cerebellar loops: motor and cognitive circuits. *Brain Res Brain Res Rev*. 2000;31:236-250.
13. Hassler R. The influence of stimulations and coagulations in the human thalamus on the tremor at rest and its physiopathologic mechanism. *Proc Second Int Congr Neuropath*. 1955:637-642.
14. Goldman MS, Ahlskog JE, Kelly PJ. The symptomatic and functional outcome of stereotactic thalamotomy for medically intractable essential tremor. *J Neurosurg*. 1992;76:924-928.
15. Benabid AL, Pollak P, Gao D, Hoffmann D, Limousin P, Gay E, et al. Chronic electrical stimulation of the ventralis intermedius nucleus of the thalamus as a treatment of movement disorders. *J Neurosurg*. 1996;84:203-214.
16. Schuurman PR, Bosch DA, Bossuyt PM, Bonsel GJ, van Someren EJ, de Bie RM, et al. A comparison of continuous thalamic stimulation

- and thalamotomy for suppression of severe tremor. *N Engl J Med.* 2000;342:461-468.
17. Campbell AM, Glover J, Chiang VL, Gerrard J, Yu JB. Gamma knife stereotactic radiosurgical thalamotomy for intractable tremor: a systematic review of the literature. *Radiother Oncol.* 2015;114:296-301.
 18. Kondziolka D, Ong JG, Lee JY, Moore RY, Flickinger JC, Lunsford LD. Gamma Knife thalamotomy for essential tremor. *J Neurosurg.* 2008;108:111-117.
 19. Witjas T, Carron R, Azulay JP, Regis J. Gamma-knife Thalamotomy for Intractable Tremors: Clinical Outcome and Correlations with Neuroimaging Features. Paper presented at: MDS 17th International Congress of Parkinson's Disease and Movement Disorders. June 16–20, 2013; Sydney, Australia.
 20. Elias WJ, Lipsman N, Ondo WG, Ghanouni P, Kim YG, Lee W, et al. A randomized trial of focused ultrasound thalamotomy for essential tremor. *N Engl J Med.* 2016;375:730-739.
 21. Benito-León J, Louis ED, Romero JP, Hernández-Tamames JA, Manzaneado E, Álvarez-Linera J, et al. Altered functional connectivity in essential tremor: a resting-state fMRI study. *Medicina.* 2015;94:e1936.
 22. Buijink AW, van der Stouwe AM, Broersma M, Sharifi S, Groot PF, Speelman JD, et al. Motor network disruption in essential tremor: a functional and effective connectivity study. *Brain.* 2015;138:2934-2947.
 23. Fang W, Chen H, Wang H, Zhang H, Puneet M, Liu M, et al. Essential tremor is associated with disruption of functional connectivity in the ventral intermediate Nucleus—Motor Cortex—Cerebellum circuit. *Hum Brain Mapp.* 2016;37:165-178.
 24. Lenka A, Bhalsing KS, Panda R, Jhunjhunwala K, Naduthota RM, Saini J, et al. Role of altered cerebello-thalamo-cortical network in the neurobiology of essential tremor. *Neuroradiology.* 2017;59:157-168.
 25. Biswal B, Yetkin FZ, Haughton VM, Hyde JS. Functional connectivity in the motor cortex of resting human brain using echo-planar MRI. *Magn Reson Med.* 1995;34:537-541.
 26. Fox MD, Greicius M. Clinical applications of resting state functional connectivity. *Front Syst Neurosci.* 2010;4:19.
 27. Morel A, Magnin M, Jeanmonod D. Multi-architectonic and stereotactic atlas of the human thalamus. *J Comp Neurol.* 1997;387:588-630.
 28. Battistella G, Najdenovska E, Maeder P, Ghazaleh N, Daducci A, Thiran JP, et al. Robust thalamic nuclei segmentation method based on local diffusion magnetic resonance properties. *Brain Struct Funct.* 2017;222:2203-2216.
 29. Witjas T, Carron R, Krack P, Eusebio A, Vaugoyeau M, Hariz M, et al. A prospective single-blind study of Gamma Knife thalamotomy for tremor. *Neurology.* 2015;85:1562-1568.
 30. Fang W, Chen H, Wang H, Zhang H, Liu M, Puneet M, et al. Multiple resting-state networks are associated with tremors and cognitive features in essential tremor. *Mov Disord.* 2015;30:1926-1936.
 31. Bain PG, Findley LJ, Atchison P, Behari M, Vidalhet M, Gresty M, et al. Assessing tremor severity. *J Neurol Neurosurg Psychiatry.* 1993;56:868-873.
 32. Fahn S, Tolosa E, Marin C. Clinical rating scale for tremor. In: Jankovic J, Tolosa E, eds. *Parkinson's Disease and Movement Disorders.* Baltimore: Urban and Schwarzenberg; 1988:225-234.
 33. Schmidt R, Freidl W, Fazekas F, Reinhart B, Grieshofer P, Koch M, et al. The Mattis Dementia Rating Scale: normative data from 1,001 healthy volunteers. *Neurology.* 1994;44:964-966.
 34. Power JD, Barnes KA, Snyder AZ, Schlaggar BL, Petersen SE. Spurious but systematic correlations in functional connectivity MRI networks arise from subject motion. *NeuroImage.* 2012;59:2142-2154.
 35. Song XW, Dong ZY, Long XY, Li SF, Zuo XN, Zhu CZ, et al. REST: a toolkit for resting-state functional magnetic resonance imaging data processing. *PLoS One.* 2011;6:e25031.
 36. Najdenovska E, Tuleasca C, Bloch J, Maeder P, Girard N, Witjas T, et al. Exploring local diffusion MRI properties for vim localization: evaluation in clinical cases. *J Neurol Surg A Cent Eur Neurosurg.* 2017;78:S1-S22.
 37. Regis J, Carron R, Park M. Is radiosurgery a neuromodulation therapy? A 2009 Fabrikant award lecture. *J Neurooncol.* 2010;98:155-162.
 38. Logothetis NK, Pauls J, Augath M, Trinath T, Oeltermann A. Neurophysiological investigation of the basis of the fMRI signal. *Nature.* 2001;412:150-157.
 39. Hipp JF, Siegel M. BOLD fMRI correlation reflects frequency-specific neuronal correlation. *Curr Biol.* 2015;25:1368-1374.
 40. Zhuge W, Ben-Galim P, Hipp JA, Reitman CA. Efficacy of MRI for assessment of spinal trauma: correlation with intraoperative findings. *J Spinal Disord Tech.* 2015;28:147-151.
 41. Fox MD, Corbetta M, Snyder AZ, Vincent JL, Raichle ME. Spontaneous neuronal activity distinguishes human dorsal and ventral attention systems. *Proc Natl Acad Sci USA.* 2006;103:10046-10051.
 42. Vossel S, Geng JJ, Fink GR. Dorsal and ventral attention systems: distinct neural circuits but collaborative roles. *Neuroscientist.* 2014;20:150-159.
 43. Gallea C, Popa T, García-Lorenzo D, Valabregue R, Legrand AP, Marais L, et al. Intrinsic signature of essential tremor in the cerebello-frontal network. *Brain.* 2015;138:2920-2933.
 44. Muthuraman M, Heute U, Deuschi G, Raethjen J. The central oscillatory network of essential tremor. *Conf Proc IEEE Eng Med Biol Soc.* 2010;2010:154-157.
 45. Borich MR, Brodie SM, Gray WA, Ionta S, Boyd LA. Understanding the role of the primary somatosensory cortex: opportunities for rehabilitation. *Neuropsychologia.* 2015;79:246-255.
 46. Cerasa A, Passamonti L, Novellino F, Salsone M, Gioia MC, Morelli M, et al. Fronto-parietal overactivation in patients with essential tremor during Stroop task. *Neuroreport.* 2010;21:148-151.
 47. Zhang J, Wang ZI, Baker KB, Vitek JL. Effect of globus pallidus internus stimulation on neuronal activity in the pedunculopontine tegmental nucleus in the primate model of Parkinson's disease. *Exp Neurol.* 2012;233:575-580.
 48. Arkadir D, Louis ED. The balance and gait disorder of essential tremor: what does this mean for patients? *Ther Adv Neurol Disord.* 2013;6:229-236.
 49. Menon V, Uddin LQ. Saliency, switching, attention and control: a network model of insula function. *Brain Struct Funct.* 2010;214:655-667.
 50. Srivardhan D, Levitin DJ, Menon V. A critical role for the right fronto-insular cortex in switching between central-executive and default-mode networks. *Proc Natl Acad Sci USA.* 2008;105:12569-12574.
 51. Roland PE, Larsen B, Lassen NA, Skinhøj E. Supplementary motor area and other cortical areas in organization of voluntary movements in man. *J Neurophysiol.* 1980;43:118-136.
 52. Jang C, Park HJ, Chang WS, Pae C, Chang JW. Immediate and longitudinal alterations of functional networks after thalamotomy in essential tremor. *Front Neurol.* 2016;7:184.
 53. Park HJ, Pae C, Friston K, Jang C, Razi A, Zeidman P, et al. Hierarchical dynamic causal modeling of resting-state fMRI reveals longitudinal changes in effective connectivity in the motor system after thalamotomy for essential tremor. *Front Neurol.* 2017;8:346.
 54. Hagmann P, Cammoun L, Gigandet X, Meuli R, Honey CJ, Wedeen VJ, et al. Mapping the structural core of human cerebral cortex. *PLoS Biol.* 2008;6:e159.
 55. Honey CJ, Sporns O, Cammoun L, Gigandet X, Thiran JP, Meuli R, et al. Predicting human resting-state functional connectivity from structural connectivity. *Proc Natl Acad Sci USA.* 2009;106:2035-2040.
 56. Wintermark M, Huss DS, Shah BB, Tustison N, Drzagal TJ, Kassell N, et al. Thalamic connectivity in patients with essential tremor treated with MR imaging-guided focused ultrasound: in vivo fiber tracking by using diffusion-tensor MR imaging. *Radiology.* 2014;272:202-209.
 57. Reich MM, Brumberg J, Pozzi NG, Marotta G, Rootthans J, Åström M, et al. Progressive gait ataxia following deep brain stimulation for essential tremor: adverse effect or lack of efficacy? *Brain.* 2016;139:2948-2956.
 58. Beckmann C, DeLuca M, Devlin J, Smith S. Investigations into resting-state connectivity using

- independent component analysis. *Philos Trans R Soc Lond B Biol Sci.* 2005;360:1001-1013.
59. Calhoun VD, Adali T, Pearson GD, Pekar JJ. A method for making group inferences from functional MRI data using independent component analysis. *Hum Brain Mapp.* 2001;14:140-151.
60. Tuleasca C, Najdenovska E, Régis J, Witjas T, Girard N, Champoutry J, et al. Clinical response to Vim's thalamic stereotactic radiosurgery for essential tremor is associated with distinctive functional connectivity patterns. *Acta Neurochir (Wien).* 2018;160:611-624.
61. Guo CC, Kurth F, Zhou J, Mayer EA, Eickhoff SB, Kramer JH, et al. One-year test-retest reliability of intrinsic connectivity network fMRI in older adults. *NeuroImage.* 2012;61:1471-1483.

Conflict of interest statement: The work was supported in part by the Swiss National Science Foundation (SNSF-205321-157040), in part by the Centre d'Imagerie BioMédicale (CIBM) of the University of Lausanne (UNIL), the Swiss Federal Institute of Technology Lausanne (EPFL), the University of Geneva (UniGe), the Centre Hospitalier Universitaire Vaudois (CHUV), the Hôpitaux Universitaires de Genève (HUG), and the Leenaards and Jeantet Foundations and in part by the CHU Timone, Marseille, France.

Received 9 November 2017; accepted 9 February 2018

Citation: World Neurosurg. (2018) 113:e453-e464.

<https://doi.org/10.1016/j.wneu.2018.02.055>

Journal homepage: www.WORLDNEUROSURGERY.org

Available online: www.sciencedirect.com

1878-8750/\$ - see front matter © 2018 Elsevier Inc. All rights reserved.

SUPPLEMENTARY MATERIALS

AUTOMATED 3T DIFFUSION MRI-BASED VENTROLATERAL VENTRAL (VLV) SEGMENTATION

In the field of an automated thalamic parcellation, several research groups have explored diffusion-weighted imaging information, although mainly by using coarse diffusion features.^{1,5} Addressing this limitation, recently our group has proposed an approach based on spherical harmonics representation of the orientation distribution functions,⁶ which provides finer details of the diffusion process within a voxel. With this approach, we subdivide the thalamus, in a robust and reproducible manner, into 7 groups of nuclei closely matching the anatomy by the Morel's atlas.⁷ Among those 7 groups is the VLV thalamic part, which encompasses in its vast surface majority the ventrointermediate nucleus and therefore is used as a region of interest in the presented study.

The thalamic mask, required for the parcellation, was first obtained from FreeSurfer (Massachusetts General Hospital, Boston, Massachusetts, USA), cortical and subcortical subdivision⁸ performed on each individual T1-weighted image and then,

according to Battistella et al.,⁶ was refined by the use of information from both the probability map representing the cerebrospinal fluid and the fractional anisotropy map.

Standard preprocessing steps were applied both for patients with essential tremor (ET; pretherapeutic, in absence of thalamotomy) and healthy controls, on diffusion-weighted imaging. In patients with ET, this included denoising, eddy current, and motion correction and in healthy control patients denoising, bias field, eddy current, and motion correction.^{6,9,10} The compensation of the echo planar imaging distortion was corrected via a nonlinear image registration between the respective T1-weighted and fractional anisotropy map using FSL FNIRT (non linear registration).⁹

An identical procedure was applied for VLV clustering for both patients with ET and healthy controls, as reported by Battistella et al.⁶ The orientation distribution function coefficients for the final thalamic subdivision, which provided the used VLV cluster, were calculated with FSL's qboot function using maximum spherical harmonics order of 66. The clustering itself was done using the modified k-means framework⁶ for each subject in its individual diffusion-image space.

REFERENCES

1. Behrens TE, Johansen-Berg H, Woolrich MW, Smith SM, Wheeler-Kingshott CA, Boulby PA, et al. Non-invasive mapping of connections between human thalamus and cortex using diffusion imaging. *Nat Neurosci*. 2003;6:750-757.
2. Deoni SC, Rutt BK, Parrent AG, Peters TM. Segmentation of thalamic nuclei using a modified k-means clustering algorithm and high-resolution quantitative magnetic resonance imaging at 1.5 T. *Neuroimage*. 2007;34:117-126.
3. Mang SC, Busza A, Reiterer S, Grodd W, Klose AU. Thalamus segmentation based on the local diffusion direction: a group study. *Magn Reson Med*. 2012;67:118-126.
4. Wiegell MR, Tuch DS, Larsson HB, Wedeen VJ. Automatic segmentation of thalamic nuclei from diffusion tensor magnetic resonance imaging. *Neuroimage*. 2003;19:391-401.
5. Zivan U, Tuch D, Westin CR. Segmentation of thalamic nuclei from DTI using spectral clustering. *Med Image Comput Assist Interv*. 2006;4191:807-814.
6. Battistella G, Najdenovska E, Maeder P, Ghazaleh N, Daducci A, Thiran JP, et al. Robust thalamic nuclei segmentation method based on local diffusion magnetic resonance properties. *Brain Struct Funct*. 2017;222:2203-2216.
7. Morel A, Magnin M, Jeanmonod D. Multi-architectonic and stereotactic atlas of the human thalamus. *J Comp Neurol*. 1997;387:588-630.
8. Fischl B, Salat DH, Busa E, Albert M, Dieterich M, Haselgrave C, et al. Whole brain segmentation: automated labeling of neuroanatomical structures in the human brain. *Neuron*. 2002;33:341-355.
9. Smith SM, Jenkinson M, Woolrich MW, Beckmann CF, Behrens TE, Johansen-Berg H, et al. Advances in functional and structural MR image analysis and implementation as FSL. *Neuroimage*. 2004;23(suppl 1):S208-219.
10. Zhang Y, Brady M, Smith S. Segmentation of brain MR images through a hidden Markov random field model and the expectation-maximization algorithm. *IEEE Trans Med Imaging*. 2001;20:45-57.